http://dx.doi.org/10.5935/0103-5053.20150044

*J. Braz. Chem. Soc.*, Vol. 26, No. 5, 851-859, 2015.
Printed in Brazil - ©2015 Sociedade Brasileira de Química
0103 - 5053 $6.00+0.00

Article

# Molecular Electronic Topology and Fragmentation Onset via Charge Partition Methods and Nuclear Fukui Functions: 1,1-Diamino-2,2-dinitroethylene

***Tiago Giannerini and Itamar Borges Jr.****

*Departamento de Química, Instituto Militar de Engenharia,*
*Praça General Tibúrcio, 80, 22290-270 Rio de Janeiro-RJ, Brazil*

We investigated theoretically the ground state electronic structure and the onset of molecular fragmentation of 1,1-diamino-2,2-dinitroethylene (FOX-7) using density functional theory. The molecular charge density was analyzed via two partition methods: the distributed multipole analysis (DMA) and the deformed atoms in molecules (DAM). In this framework, the push-pull effect, hydrogen intra-molecular bonding and site acid-base properties of the molecule were discussed. Our analysis indicates that the molecular origin of the low measured impact sensitivity of FOX-7 is due to the magnitude of multipole values of the C–N bonds in the $NO_2$ groups, the delocalized electrons over the central C–C bond and the hydrogen bonds. The onset of FOX-7 decomposition and acid-base properties were examined with the nuclear Fukui functions. The results support nitro to nitrite rearrangement and direct release of a $NO_2$ as a possible initial step in FOX-7 decomposition process. The approach suggested is general and can be especially useful for very large molecules to examine in detail their electronic structure and to guide the search for the decomposition mechanisms.

**Keywords:** molecular charge partition methods, conceptual DFT, nuclear Fukui functions, molecular fragmentation, energetic materials, FOX-7, DADNE

## Introduction

A complete investigation of the ground state properties of a molecule or a solid in the framework of density functional theory (DFT) can be achieved in principle from the knowledge of the quantum observable electron density; when the nuclei charges are included it is the charge distribution.[1] A very convenient way to analyze those densities is by employing a physically and chemically justified method to divide them into atomic contributions.

Methods that divide molecular charge densities into atomic contributions belong to a large family of charge density analysis approaches that provides detailed knowledge of topological bonding properties. These methods have undergone "a major renaissance in the last two decades" according to a recent review.[2] A textbook on the subject with authoritative reviews has just been edited.[3]

The key idea of what is known as conceptual DFT is treating the response of a system to a perturbation as determining its reactivity, in this way providing an interpretative approach to a diversity of chemistry phenomena.[4-13] These response functions are derivatives of the energy with respect to a perturbation that can be interpreted as reactivity indicators. According to conceptual DFT, fragmentation of the energetic material 1,3,5-trinitro-1,3,5-triazacyclohexane (RDX) was studied successfully with nuclear Fukui functions used as reactivity indicators.[14-16]

Development of new energetic materials has the dual purpose of combining large release of energy (good performance) and great resistance to impact or friction (low impact sensitivity). There are several relevant and interesting issues related to the quantum chemistry research of energy-rich materials, and an important book on the subject has just been released.[17]

The recently synthesized 1,1-diamino-2,2-dinitroethylene,[18] FOX-7 or DADNE, when compared to the widely used explosive RDX,[16] exhibits similar performance but a much lower sensitivity to impact. This new explosive is still not widely used due to its large production costs. FOX-7 is also a promising precursor in organic chemistry and despite its simple structure, this molecule has very unusual properties. We explored lately the excited states of this molecule.[19] However, most works on this system are

*e-mail: itamar@ime.eb.br

oriented to applications and do not approach systematically fundamental issues,[20] an important motivation of this work.

FOX-7 has an electronic push-pull effect as the result of one side of the molecule bearing two electron-withdrawing nitro groups as a strong oxidation center whereas the other side has two electron-donating amino groups.[20] Politzer *et al.*,[21] using B3P86/6-31+G**, assessed the role of "push-pull" electronic delocalization and intramolecular hydrogen bonding effects in FOX-7 and analogous compounds according to the bond lengths in the inner skeleton of the molecules. Due to the push-pull effect, the electron distribution of FOX-7 is unbalanced.

There are three possible unimolecular decomposition mechanisms of FOX-7:[20,22-26] (*i*) nitro-nitrite rearrangement followed by NO release, (*ii*) direct cleavage of the C–$NO_2$ bond and, (*iii*) intra/intermolecular hydrogen transfer followed by HONO release. Gindulyte *et al.*,[22] using DFT calculations with the B3LYP and B3P86 hybrid functionals and the 6-31+G(d,p) Gaussian basis set, proposed that nitro-nitrite rearrangement is the most probable outcome. They based the suggestion on the computation of an energy barrier of 59.1 kcal $mol^{-1}$ (B3LYP) for this step, in very good agreement with the measured activation energy value of 58 kcal $mol^{-1}$.[27] However, because their C–$NO_2$ dissociation value is only ca. 15 kcal $mol^{-1}$ higher, this process cannot be discarded for two reasons: in view of the involved energies in the decomposition of an energetic material and because the direct bond cleavage is a rather common process in these materials. Rashkeev *et al.*[23] combined DFT calculations and periodic boundary conditions (PBC) in the generalized gradient approximation (GGA) to conclude that the direct C–$NO_2$ rupture hypothesis is more plausible. They found a bond dissociation energy of 92 kcal $mol^{-1}$ for a perfect crystal, reduced to 59 kcal $mol^{-1}$ by considering common crystal defects. Kimmel *et al.*[24-26] used DFT and embedded cluster methods to propose that intra or intermolecular hydrogen transfer is not a feasible initiation step of FOX-7 decomposition. Instead, both C–$NO_2$ bond fission and nitro-nitrite rearrangement would be the competing mechanisms. In this work, we examine the onset of molecular FOX-7 fragmentation and discuss the three possible pathways through nuclear Fukui functions.

Concerning impact sensitivity of energetic materials, there have been several theoretical attempts to establish relationships between this important macroscopic property and different molecular characteristics.[28-39] Zaho-Xu and Chen[40] have just published a comprehensive account of quantum chemistry derived criteria for impact sensitivity and Politzer and Murray[41] discussed the challenges involved in predicting it. Among the quantum-mechanical molecular properties used to investigate impact sensitivity, we can mention electrostatic potentials (ESPs),[28-31,33,38] Mulliken charges of nitro groups,[32,34,37] and Bader's atoms in molecules (AIM) method.[42,43] According to Yau *et al.*,[43] the AIM method cannot be used to build such correlations because this space partition scheme of the electron density is very sensitive to DFT functionals and type of basis sets.

In previous works, we used the distributed multipole analysis (DMA) method to analyze charge distributions and sensitivity of energetic molecules[36,39] as well as properties of $MoS_2$ catalysts.[44-46] In contrast to the AIM approach,[43] our results showed that DMA is quite stable with respect to DFT parameters and basis set size. In another work, we used the deformed atoms in molecules (DAM) method and nuclear Fukui functions to examine the influence of charge densities in the stability and decomposition pathways of four different RDX conformers.[16] It is important to note that direct examination of the electron (charge) density is more accurate than inspection of the self-consistent field molecular orbitals because the former includes correlation effects.[9]

In other works, we investigated the excited and ionized states of energetic molecules including possible decomposition processes[47-51] and FOX-7.[19] These molecules have in common X–$NO_2$ bonds (X=N,C), a feature of widely used energetic materials.

The main purpose of this paper is to show that physical and chemically motivated molecular charge density partition methods and conceptual DFT allows one to investigate in details topological molecular properties and onset of molecular fragmentation. We applied this approach to the FOX-7 molecule to analyze push-pull effects, hydrogen bonds, impact sensitivity, site properties and decomposition mechanisms.

## Methodology

The ground state geometry of FOX-7 was optimized with the hybrid functional B3LYP[52] and the aug-cc-pVTZ Gaussian basis set.[53,54] Frequency calculations confirmed the minimum character of the structure. The calculations were made with the Gaussian 03 package.[55]

The computed DFT electron density was decomposed according to the DMA using the GDMA2 software.[56] For the DAM analysis, we used the DAMQT program.[57] The Hellmann-Feynman forces, obtained from the DAM analysis, were combined to calculate the $G_i$ and $\Phi_i$ nuclear Fukui vectors. The DMA molecular pictures were prepared with the graphic program Gabedit.[58]

The DMA and DAM molecular partition methods, including the chemical concepts involved, are discussed in the Supplementary Information (SI) section.

From the DAM partition of the electron density, one can compute the nuclear Fukui functions to analyze site properties and the onset of molecular fragmentation.[4,14-16,59,60] The idea of nuclear Fukui functions stems from the Hellmann-Feynman electrostatic theorem.[61] According to it, the total electrostatic force $\mathbf{F}_i$ on a nucleus *i* in a molecule due to the electrons and the remaining nuclei is given in atomic units by

$$\mathbf{F}_i = \left[ Z_i \int \rho(\mathbf{r}) \frac{\mathbf{r}_i}{r_i^3} d^3r - \sum_{i \neq j} Z_j \frac{\mathbf{R}_{ij}}{R_{ij}^3} \right] \quad (1)$$

where $\rho(\boldsymbol{r})$ is the electron density at position $\mathbf{r}$, $\mathbf{r}_i$ is the separation vector between nucleus *i* and position $\mathbf{r}$ and $\mathbf{R}_{ij}$ is the separation vector between nuclei *i* and *j* with $Z_i$ and $Z_j$ charges, respectively. From the Hellmann-Feynman forces, Ordon and Komorowski[59,60] define two nuclear Fukui response functions. One is the derivative of electronegativity ($\chi$) over the nuclei distortion $\boldsymbol{Q}_i$, called nuclear reactivity $\boldsymbol{\Phi}_i$:

$$\Phi_i = \frac{\partial \chi}{\partial Q_i} \cong \frac{1}{2}\left(F_i^+ - F_i^-\right) \quad (2)$$

The other is the derivative of hardness ($\boldsymbol{\eta}$) over the atomic displacements $\boldsymbol{Q}_i$, the nuclear stiffness $\mathbf{G}_i$:

$$G_i = \frac{\partial \eta}{\partial Q_i} \cong -\frac{1}{2}\left(F_i^+ + F_i^-\right) \quad (3)$$

The Hellmann-Feynman forces $\mathbf{F}^+$ and $\mathbf{F}^-$ are the total forces acting on the $i^{th}$ nucleus when one electron is added or removed, respectively, and are computed at the geometry of the neutral system. The nuclear Fukui functions are then calculated from the above finite differences. The $\mathbf{G}_i$ and $\boldsymbol{\Phi}_i$ functions are intrinsic molecular properties and form a set of vectors in 3D space with origin on each atomic nuclei. Their components and magnitude for each atom are reported in Table S1 in the SI section.

## Results and Discussion

### Geometry

Figure 1 shows the B3LYP/aug-cc-pVTZ optimized structure. The main geometric parameters are presented in Table 1. The results are compared with X-ray data of Bemm *et al.*[62] and theoretical values of Sorescu *et al.*[63] and Gindulyte *et al.*[22] Sorescu *et al.*[63] used PBC and the Perdew-Wang 86 GGA functional whereas Gindulyte *et al.*[22] examined the isolated molecule using B3P86/6-31G+(d,p). The calculations of Sorescu *et al.*[63] and the experimental results of Bemm[62] were obtained for a crystal. For this reason, the corresponding columns in Table 1 can have two values.

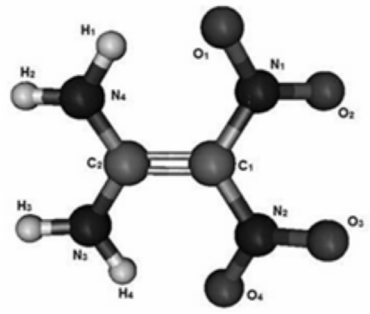


**Figure 1.** B3LYP/aug-cc-pVTZ optimized geometry of FOX-7 molecule.

The overall agreement is very good. Not surprisingly, the largest difference for the isolated molecule results concerns the $N_1$–$C_1$–$C_2$–$N_4$ dihedral angle. Our angle value is closer to experiment as compared to the results of Gindulyte *et al.*,[22] but it is still about 6° larger as compared to measurements and PBC results. In gas phase, the molecule has greater freedom, so a different value of the torsional angle is expected. The reason for this non-planarity is the repulsion between the oxygen atoms of the nitro groups. Sorescu *et al.*[63] also performed MP2/6-31+G** and B3LYP/6-31+G** calculations and obtained a value of 16° for the dihedral angle, still farthest from experiment and our value.

### Analysis of molecular charge densities and derived properties

Figure 2a depicts the DMA multipoles centered on the FOX-7 sites. The DMA dipole vectors in FOX-7 (Figure 2a) clearly display the inductive over the entire molecule, with the vector components directed towards the electron withdrawing nitro groups, thus indicating the dislocation of electron density towards them. Furthermore, the size of the dipole vectors on distinct sites, combined with the charge and quadrupole values, indicate the local magnitude of the inductive effect and could be used to quantify it among different molecules. The large values of the site quadrupole moment on both carbon atoms, especially on $C_1$, which is bonded to the two nitro groups, imply delocalized ($\pi$) electrons over the C–C bond. This picture of charge distribution due to the presence of high electron density withdrawing groups on one side of a double bond and donating groups on the other side results is the so-called push-pull effect.[21,64]

The large quadrupole values on the oxygen atoms of the nitro groups and on the nitrogen atoms of the

**Table 1.** Computed FOX-7 geometric parameters for FOX-7 and literature values

| | Present work | Gindulyte *et al.*[22] | Sorescu *et al.*[a,63] | Bemm *et al.*[b,62] (exp.) |
|---|---|---|---|---|
| | | Distance / Å | | |
| $C_1$–$C_2$ | 1.422 | 1.426 | 1.465 | 1.459 |
| $C_1$–N ($NO_2$) | 1.431 | 1.424 | 1.423/1.410 | 1.427/1.398 |
| $C_2$–N ($NH_2$) | 1.339 | 1.339 | 1.336/1.331 | 1.325/1.319 |
| $N_1$–$O_1$ | 1.249 | 1.251 | 1.271/1.264 | 1.249/1.242 |
| $N_1$–$O_2$ | 1.215 | 1.219 | 1.262 /1.262 | 1.242/1.242 |
| $N_4$–$H_1$ | 1.013 | 1.019 | 1.018/1.019 | 0.840/0.871 |
| $N_4$–$H_2$ | 1.004 | 1.007 | 1.024/1.022 | 0.882/0.838 |
| $O_1$–$H_1$ | 1.800 | – | 1.880 | 1.970 |
| | | Angle / degrees | | |
| $C_1$–$C_2$–$N_4$ | 121.3 | 121.1 | 120.70/121.04 | 120.72/120.82 |
| $N_1$–$C_1$–$C_2$ | 121.7 | 121.6 | 119.85/123.46 | 119.74/123.89 |
| $N_3$–$C_2$–$N_4$ | 117.4 | 117.8 | 118.22 | 118.42 |
| $N_1$–$C_1$–$N_2$ | 116.7 | 116.9 | 116.68 | 116.32 |
| | | Torsion of the molecular plane / degrees | | |
| $N_1$–$C_1$–$C_2$–$N_4$ | 11.64 | ca. 20 | 4.86 | 4.68 |

[a]Some geometric parameters have two distinct computed values. See text for details; [b]some geometric parameters have two distinct measured values. See text for details.

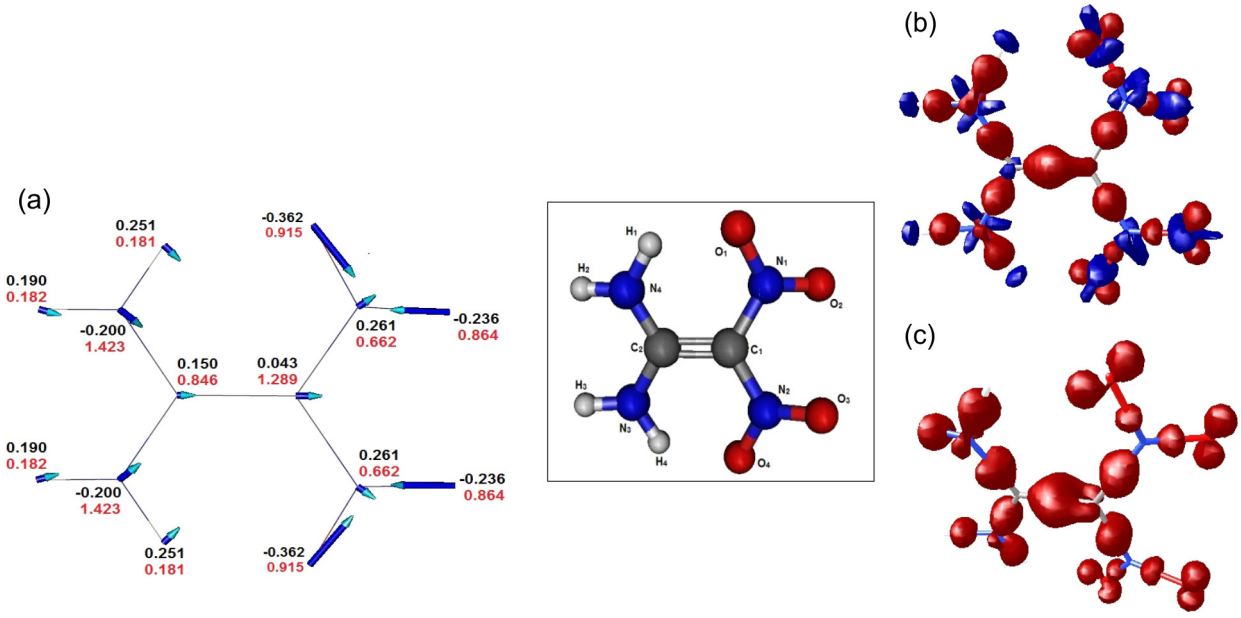


**Figure 2** (a) FOX-7 computed DMA multipole values. Numbers written in the upper position of each site are monopole values (black) in units of $e$ ($1.602 \times 10^{-19}$ C). Those in the lower position (red) are the quadrupole values in ($4.486 \times 10^{-40}$ C m$^2$) units. Site dipoles are represented by vectors drawn at the corresponding atomic nuclei. (b) FOX-7 DAM regions of electron accumulation (red) and depletion (blue). In panel (c), the depletion regions were omitted. DAM boundary values equal ± 0.030 a.u. (electron bohr$^{-3}$).

amine groups are due to their lone pairs. The oxygen atoms in the nitro groups have different types of charge separation depending on the position, as expressed by the DMA and DAM results displayed in Figure 2. The $O_2$ and $O_3$ oxygen atoms, localized at the far right of FOX-7 (Figure 2), have their dipole vectors aligned with the N–O bond axis, opposing charge separation from the corresponding nitrogen atom. The same situation, but of larger magnitude, also occurs on the $O_1$ and $O_4$ atoms although dipole vectors in this case are no longer totally aligned with the N–O bond. This charge separation-bond polarization effect seems rather general.[65] Furthermore,

the $O_2$ and $O_3$ oxygen atoms have different values of the charge and quadrupole values as compared to the $O_1$ and $O_4$ corresponding ones due to the intra-hydrogen bonds formed by $O_2$ and $O_3$, as discussed below.

The $O_1$ and $O_4$ negative charge, dipole and quadrupole values are larger compared with the corresponding values on the $O_2$ and $O_3$ atoms. These larger multipole values result from the attractive electrostatic interaction between the $H_1$ and $O_1$ atoms and between $H_4$ and $O_4$. Due to this interaction, the $O_1$ and $O_4$ atoms display more negative charge in the corresponding nitro group in comparison with the other two oxygen atoms, $O_2$ and $O_3$, farthest from the hydrogen atoms in the molecule. This attractive electrostatic interaction between the charges of the $H_1$---$O_1$ and $H_4$---$O_4$ pairs is characteristic of hydrogen bonds[66] and the DMA multipole values allows one to quantify their strengths in an electrostatic picture.

In FOX-7 there is also the displacement of electrons on the $N_3$–$H_3$ and $N_4$–$H_2$ bonds involved in the hydrogen bonds. These displacements are seen as a bump of electron accumulation (red) on the middle of the bonds computed according to the DAM method (Figures 2b and 2c). In the amine groups, the electron depletion regions (blue) on the $H_1$ and $H_4$ atoms correspond to DMA positive charges and small quadrupole values, whereas the $N_3$ and $N_4$ atoms have negative charges and large quadrupole values. The latter are more than twice as large as compared to the corresponding values on the nitrogen atoms ($N_1$ and $N_2$) of the nitro groups.

The other partition approach, the DAM method, highlights pictorially the above results. In Figures 2b and 2c, charge accumulation along the C–C bond in FOX-7 is displaced towards the carbon atom $C_1$, with a bump around the middle of the bond. Therefore, the $C_1$ atom displays a larger electron accumulation as compared with $C_2$; in fact, Figure 2b shows a region of electron depletion (blue) over $C_2$. In the DAM method, electron accumulation in a double bond is observed as an out-of-plane deformation of the electron accumulation region (red) over the C–C bond (Figures 2b and 2c). This picture is also confirmed by the large value of the corresponding $C_1$ and $C_2$ DMA quadrupole moment values (Figure 2a).

The results just discussed can be related to the low impact sensitivity of FOX-7. For molecules having $NO_2$ groups, this property is connected to the feasibility of breaking the C–$NO_2$ out C –$NO_2$ bonds, the so called trigger linkage.[40,41,67] The "trigger" bonds are the ones likely to be broken by an external stimulus having the necessary energy. These bond ruptures then trigger the further exothermic and self-sustaining decomposition processes that characterizes the detonation or explosion.[41] In another work, we confirmed the already existing indications that charge values on the nitro groups are directly related to the impact sensitivity.[39] Moreover, we showed that explosives with large delocalized electron densities and positive charge values on the aromatic ring of nitroaromatics correspond to more insensitive materials. Politzer *et al.*,[41,68] by examining the molecular electrostatic potential in different investigations, identified that the balance between charge delocalization and $NO_2$ electron-withdrawing is determinant for the impact sensitivity of an energetic material. Our results[39] also agreed with the work of Rice and Hare[30] that associated the magnitude of sensitivity to impact to the degree of positive charge build-up (i.e., electron deficiency) over covalent bonds within the inner framework of explosives. Therefore, very sensitive explosives display large electron depletion over the covalent bonds of the molecules whereas the insensitive ones do not have it.

The impact sensitivity of FOX-7 can be discussed according to the ideas of the last paragraph. In FOX-7, the C=C bond can be thought to play the role of the central structure of the molecule (i.e., as the aromatic ring in nitroaromatics). The carbon atoms have large DMA quadrupole values (Figure 2a), thus large delocalized electron densities; both carbon atoms also have positive charge values. Furthermore, note that: (*i*) the quadrupole values on the N atom localized in the nitro groups are about half the values on the N atoms in the amine groups and, (*ii*) the charge values are positive on the N atoms of the nitro groups in contrast with the negative values on the N atoms of the amines. Therefore, because the charges on the carbon atoms are positive, in the framework of the Coulombic charge bond model (see SI section), the strength of the C–$NO_2$ bonds are about 3 times smaller and of repulsive nature when compared with the C–$NH_2$ bonds. Moreover, from a purely electrostatic view, the C–$NO_2$ bonds are repulsive (both charges are positive) whereas the C–$NH_2$ bonds are attractive. Therefore, the barriers to break the C–$NO_2$ bonds should be smaller when compared to the C–$NH_2$ bonds, as they are in fact.[41]

We showed above that in FOX-7 there is an overall charge delocalization and unbalance provoked by the two electron-donating amino groups and the two electron-acceptor nitro groups. The presence of electron-donating amino groups tends to diminish the impact sensitivity. Moreover, the inter- and intra-molecular hydrogen bonding in FOX-7 not just stabilize the system, but may increase thermal conductivity that can promote diffusion and dissipation of hot spot energy (i.e., small regions of the crystal lattice where part of the energy coming from an external stimulus is localized and can initiate the

self sustaining exothermal chemical decomposition).[41] Therefore, all the aforementioned molecular properties imply that FOX-7 is rather insensitive, as it is in fact.

We now discuss qualitatively acid-base site properties.

The region around the $C_1$ atom is by far the one with the greatest electron accumulation in the molecule (Figures 2b and 2c), being, for this reason, the main Lewis basic site of FOX-7. This site has also (Figure 2a) a large value of the DMA quadrupole moment and almost null values of DMA charge and dipole, another indication of electron accumulation in the region. This behavior is confirmed in halogenation and nitration electrophilic reactions:[20] in the first reaction step, the strong electrophiles $Cl^+$, $Br^+$ and $NO_2^+$ attack the $C_1$ carbon atom. Therefore, the $C_1$ site has electrophilic character.

In the first report of FOX-7 synthesis,[18] a low nucleophilicity of the amino groups was found. This property is confirmed by examining the region around the $C_2$ atom, where there is clearly electron depletion (Figure 2b). Moreover, this is also verified by the DMA multipoles: in comparison with the $C_1$ atom, $C_2$ has over three times a positive charge and about a 35% smaller quadrupole value (Figure 2a).

Both the large susceptibility of the $C_1$ atom to electrophilic attack and the low nucleophilicity of the $C_2$ atom are related to the push-pull behavior of FOX-7. In the next section, we show that the nuclear Fukui functions also provide similar insights on acid-base properties.

## Onset of molecular fragmentation and reactivity behavior of the carbon sites

From the Hellmann-Feynman forces, we computed the nuclear Fukui functions stiffness $\mathbf{G_i}$ and reactivity $\mathbf{\Phi_i}$. As described above, these atomic vectors indicate the most favorable displacements for the onset of molecular decomposition.

Figure 3 depicts the computed nuclear Fukui response functions of FOX-7. In Table S1, in the SI section, the component values and the total magnitude of the nuclear Fukui vectors on each site are reported.

It can be noted that both response functions in the nitro group atoms are the most prominent, especially the $\mathbf{G_i}$ vectors on the oxygen atoms. This picture agrees with the aforementioned three proposed decomposition mechanisms in the sense that a nitro group is always involved.

Both $\mathbf{\Phi_i}$ vectors on the carbon atoms are along the C–C bond and in opposite directions. However, because the magnitude of the $C_2$ $\mathbf{\Phi_i}$ vector is much larger as compared to the $C_1$ $\mathbf{\Phi_i}$ vector, by a factor of about 6, a C–C bond strengthening is much favored. On the other hand, the $C_1$ $\mathbf{G_i}$ vector magnitude as compared to the $C_2$ $\mathbf{G_i}$ value, although could seem to imply the weakening of the C–C bond, because the ratio between these $\mathbf{G_i}$ vectors is only ca. 2 and the magnitude of the $C_1$ $\mathbf{\Phi_i}$ vector is the largest of the vectors on the carbon atoms (see Table S1), this is not so. Therefore, as expected, the strength of the C–C bond is large and the decomposition processes in FOX-7 do not involve its cleavage.

The typical dissociation process of nitro-containing compounds is the cleavage of a $N–NO_2$ or $C–NO_2$ bond.[22,51] The $C–NH_2$ bond is known to have a very high dissociation energy;[22] note the very small magnitudes of the corresponding response function vectors (Figure 3 and Table S1) and its large bond strength according to the Coulombic model discussed above. Previous analysis of nuclear Fukui functions for the RDX decomposition[14-16] indicates that onset of decomposition in 3 out of 4 conformers was a direct $N–NO_2$ bond dissociation. In RDX, the nuclear reactivity $\mathbf{\Phi_i}$ vectors of the two nitrogen atoms in the $NO_2$ groups point to opposite directions, away from each other and outwards the molecule. In contrast to RDX, in FOX-7 the reactivity vector $\mathbf{\Phi_i}$ on the nitrogen atom of each nitro group implies a NO bond

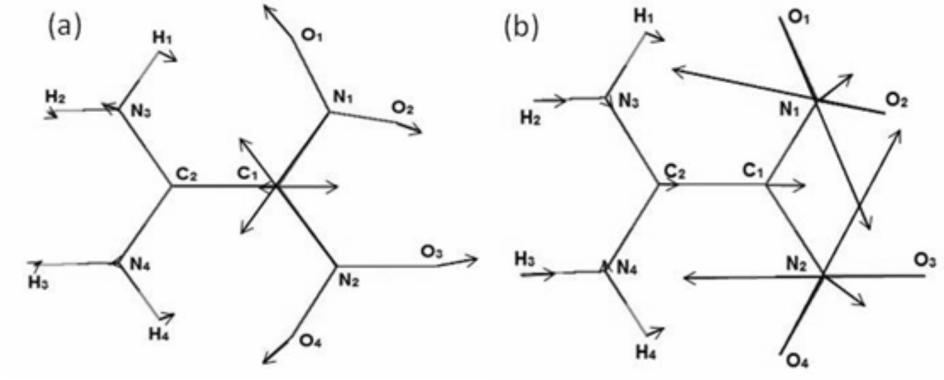


**Figure 3.** Computed nuclear Fukui functions determined as vectors for each atomic site. (a) Nuclear reactivity vectors $\mathbf{\Phi_i}$ and (b) the nuclear stiffness vectors $\mathbf{G_i}$. The vectors are not to scale between the different panels.

length decrease, thus a strengthening of the C–N bonds. Conversely, the projection of the nitrogen $\mathbf{G_i}$ vectors over the C–N bonds indicates their stretch, thus their weakening leading to the possibility of a direct $NO_2$ dissociation. However, because the magnitude of the nitrogen $\mathbf{G_i}$ vectors is ca. 12% larger as compared to the corresponding $\mathbf{\Phi_i}$ vectors, the direct $NO_2$ release is favored over the converse (Table S1).

According to the overall distribution of the $\mathbf{\Phi_i}$ vectors, especially the large vectors on the oxygen atoms, the rearrangement path (nitro-to-nitrite) is also possible. The $\mathbf{G_i}$ nuclear stiffness vectors of FOX-7 oxygen atoms are much larger than all the others in the molecule including the $\mathbf{\Phi_i}$ vectors (Table S1), a picture also supporting the rearrangement path (Figure 4b). Therefore, there is an appreciable probability of oxygen atoms being involved in the onset of a fragmentation reaction, thus reinforcing the idea that a rearrangement process may be the most probable decomposition pathway. However, as discussed above, the $\mathbf{G_i}$ vectors in the $N_1$ and $N_2$ atoms points outwards this way, also implying the possibility of direct C–$NO_2$ bond breaking as happens in RDX, nitroethylene and other energetic molecules having the explosophore $NO_2$ groups. The third possible decomposition process, the intramolecular hydrogen transfer followed by HONO release, according to the very small magnitude of the $\mathbf{\Phi_i}$ and $G_i$ vectors on the $H_1$ and $H_4$ hydrogen atoms, is very unlikely.

The reactivity behavior of the carbon sites can also be examined with the nuclear Fukui functions. The largest carbon $\mathbf{\Phi_i}$ vector is on the $C_2$ atom, which is bonded to the amine group. This large value of the $\mathbf{\Phi_i}$ vector indicates a large variation of the site electronegativity, thus the $C_2$ atom is a better electron acceptor site as compared to $C_1$. Therefore, as experimentally verified before[18,20] and seen above with the partition methods, the $C_2$ site is a better electron acceptor, thus has a small nucleophilicity.

Conversely, the large $\mathbf{G_i}$ vector on the $C_1$ site indicates a large variation of the site hardness, thus electron acceptance is hindered. Therefore, attack of strong electrophiles is very favored, a property which was also experimentally verified.[18,20]

## Conclusions

The electronic structure of the energetic molecule 1,1-diamino-2,2-dinitroethylene (FOX-7) was thoroughly examined using two different partition methods, which provided a very complete and accurate picture of the topology of the molecular charge distribution. We also calculated two nuclear Fukui functions and employed them to discuss the onset of molecular fragmentation and reactivity properties.

The distribution of the DMA dipole vectors on the atomic sites showed a displacement of FOX-7 charge density towards the nitro groups, a signature of the push-pull effect. The two carbon atoms have distinct properties, a feature rationalized from the DMA quadrupole values and the DAM picture of electron accumulation; both methods showed the displacement of the electron density towards the carbon atom $C_1$, which is bonded to the nitro groups, thereby decreasing its positive charge.

We discussed how intra-molecular hydrogen bonds overall affects the charge distribution topology in FOX-7. The charge values of the hydrogen and oxygen atoms directly involved in these bonds are marked different from the ones not involved, as indicated by DMA dipole vectors and DAM regions of charge accumulation. The large DMA multipole values and the DAM electron accumulation bumps clearly represent the double-bond character of the C–C bond. We also considered the multipole values of the C–N bonds in the $NO_2$ groups. These facts explain the lower sensitivity to impact of FOX-7 and its behavior as energetic material, since the C–$NO_2$ bonds are involved in the material decomposition.

The acid-base properties of the carbon atoms, which are involved in electrophilic and nucleophilic reactions were discussed using both the decomposed charge densities and the nuclear Fukui functions. Considering the onset of decomposition, both sets of nuclear Fukui functions support a nitro to nitrite rearrangement as the initial step in the decomposition process and the possibility of a direct C–$NO_2$ bond cleavage.

In this work, we showed the wealthy of information that can be gathered concerning molecular electronic structure and the onset of fragmentation processes by combining two charge partition methods and response nuclear Fukui functions. In contrast to partition methods such as the widely used Bader's atoms in molecules (AIM) method, which divides the electronic density into regions and uses non-chemically intuitive concepts such as attractors, critical points among others, the distinct atom-centered methods used here have a clear chemical interpretations. The DMA, DAM and nuclear Fukui functions concepts were applied to the recently synthesized energetic material, 1,1-diamino-2,2-dinitroethylene molecule. Furthermore, the approach employed is general and can be especially useful for very large molecules. For these large systems, the molecular electronic structure can be examined in detail and the nuclear Fukui functions can serve as a guide for the search of decomposition mechanisms, especially in situations for which employing directly the conventional methods can be difficult.

## Supplementary Information

Supplementary information (tables of the components of the nuclear Fukui function vectors and discussion of the DMA and DAM partition methods) are available free of charge at http://jbcs.sbq.org.br as PDF file.

## Acknowledgments

We thank CNPq, CAPES, Faperj and the Brazilian Army for supporting this research. T. G. thanks Instituto Federal de Educação, Ciência e Tecnologia do Rio de Janeiro for a leave of absence to carry on this work as part of his PhD dissertation.

## References

1. Koch, W.; Holthausen, M. C.; *A Chemist's Guide to Density Functional Theory*, 2nd ed.; Wiley-VCH: Weinheim, 2002.
2. Chopra, D.; *J. Phys. Chem. A* **2012**, *116*, 9791.
3. Gatti, C.; Macchi, P.; *Modern Charge-Density Analysis*, Springer: New York, 2012.
4. Balawender, R.; De Proft, F.; Geerlings, P.; *J. Chem. Phys.* **2001**, *114*, 4441.
5. Geerlings, P.; De Proft, F.; Langenaeker, W.; *Chem. Rev.* **2003**, *103*, 1793.
6. Geerlings, P.; De Proft, F.; *Phys. Chem. Chem. Phys.* **2008**, *10*, 3028.
7. Liu, S. B.; *Acta Phys.-Chim. Sin.* **2009**, *25*, 590.
8. Martinez, J.; Toro-Labbe, A.; *J. Math. Chem.* **2009**, *45*, 911.
9. Johnson, P. A.; Bartolotti, L. J.; Ayers, P. W.; Fievez, T.; Geerlings, P.; *Charge Density and Chemical Reactions: A Unified View from Conceptual DFT Modern Charge-Density Analysis*; Gatti, C.; Macchi, P., eds.; Springer: Netherlands, 2012.
10. Geerlings, P.; Ayers, P. W.; Toro-Labbe, A.; Chattaraj, P. K.; De Proft, F.; *Acc. Chem. Res.* **2012**, *45*, 683.
11. Giri, S.; Echegaray, E.; Ayers, P. W.; Nunez, A. S.; Lund, F.; Toro-Labbe, A.; *J. Phys. Chem. A* **2012**, *116*, 10015.
12. Chakraborty, D.; Cardenas, C.; Echegaray, E.; Toro-Labbe, A.; Ayers, P. W.; *Chem. Phys. Lett.* **2012**, *539*, 168.
13. Geerlings, P.; Fias, S.; Boisdenghien, Z.; De Proft, F.; *Chem. Soc. Rev.* **2014**, *43*, 4989.
14. Luty, T.; Ordon, P.; Eckhardt, C. J.; *J. Chem. Phys.* **2002**, *117*, 1775.
15. Swadley, M. J.; Li, T. L.; *J. Chem. Theory Comput.* **2007**, *3*, 505.
16. Moraes, T. F.; Borges, I.; *Int. J. Quantum Chem.* **2011**, *111*, 1444.
17. Sabin, J. R.; *Advances in Quantum Chemistry*, *Energetic Materials, Volume 69*; Academic Press: Oxford, 2014.
18. Latypov, N. V.; Bergman, J.; Langlet, A.; Wellmar, U.; Bemm, U.; *Tetrahedron* **1998**, *54*, 11525.
19. Borges, I.; *J. Mol. Model.* **2014**, *20*, 1.
20. Simkova, L.; Liska, F.; Ludvik, J.; *Curr. Org. Chem.* **2011**, *15*, 2983.
21. Politzer, P.; Concha, M. C.; Grice, M. E.; Murray, J. S.; Lane, P.; Habibollazadeh, D.; *Theochem-Journal of Molecular Structure* **1998**, *452*, 75.
22. Gindulyte, A.; Massa, L.; Huang, L. L.; Karle, J.; *J. Phys. Chem. A* **1999**, *103*, 11045.
23. Rashkeev, S. N.; Kuklja, M. M.; Zerilli, F. J.; *Appl. Phys. Lett.* **2003**, *82*, 1371.
24. Kimmel, A. V.; Sushko, P. V.; Shluger, A. L.; Kuklja, M. M.; *J. Chem. Phys.* **2007**, *126*, 10.
25. Kimmel, A. V.; Sushko, P. V.; Shluger, A. L.; Kuklja, M. M.; *J. Phys. Chem. A* **2008**, *112*, 4496.
26. Kimmel, A. V.; Ramo, D. M.; Sushko, P. V.; Shluger, A. L.; Kuklja, M. M.; *Phys. Rev. B: Condens. Matter Mater. Phys.* **2009**, *80*, 134108.
27. Östmark, H.; Langlet, A.; Bergman, H.; Wingborg, U.; Wellmar, U.; Bemm, U.; FOX-7 – a new explosive with low sensitivity and high performance. In *11th International Symposium on Detonation*, Snow Mass, Colorado, 1998.
28. Murray, J. S.; Lane, P.; Politzer, P.; *Mol. Phys.* **1995**, *85*, 1.
29. Murray, J. S.; Lane, P.; Politzer, P.; *Mol. Phys.* **1998**, *93*, 187.
30. Rice, B. M.; Hare, J. J.; *J. Phys. Chem. A* **2002**, *106*, 1770.
31. Murray, J. S.; Concha, M. C.; Politzer, P.; *Mol. Phys.* **2009**, *107*, 89.
32. Zhang, C. Y.; Shu, Y. J.; Huang, Y. G.; Zhao, X. D.; Dong, H. S.; *J. Phys. Chem. B* **2005**, *109*, 8978.
33. Politzer, P.; Murray, J. S.; *J. Mol. Struct.* **1996**, *376*, 419.
34. Zhang, C. Y.; *Propellants, Explos., Pyrotech.* **2008**, *33*, 139.
35. Meents, A.; Dittrich, B.; Johnas, S. K. J.; Thome, V.; Weckert, E. F.; *Acta Crystallogr., Sect. B: Struct. Sci.* **2008**, *64*, 42.
36. Borges, I.; *Int. J. Quantum Chem.* **2008**, *108*, 2615.
37. Zhang, C. Y.; *J. Hazard. Mater.* **2009**, *161*, 21.
38. Pospisil, M.; Vavra, P.; Concha, M. C.; Murray, J. S.; Politzer, P.; *J. Mol. Model.* **2010**, *16*, 895.
39. Anders, G.; Borges, I.; *J. Phys. Chem. A* **2011**, *115*, 9055.
40. Chen, Z.-X.; Xiao, H.-M.; *Propellants, Explos., Pyrotech.* **2014**, *39*, 487.
41. Politzer, P.; Murray, J. S. In *Advances in Quantum Chemistry*; Sabin, J. R., ed.; Academic Press: Oxford, 2014, ch. 1.
42. Najafpour, J.; Zohari, N.; *Iran. J. Chem. Chem. Eng.* **2011**, *30*, 113.
43. Yau, A. D.; Byrd, E. F. C.; Rice, B. M.; *J. Phys. Chem. A* **2009**, *113*, 6166.
44. Borges, I.; Silva, A. M.; Aguiar, A. P.; Borges, L. E. P.; Santos, J. C. A.; Dias, M. H. C.; *J. Mol. Struct.: THEOCHEM* **2007**, *822*, 80.
45. Silva, A. M.; Borges, I.; *J. Comput. Chem.* **2011**, *32*, 2186.

46. Borges, I.; Silva, A. M.; *J. Braz. Chem. Soc.* **2012**, *23*, 1789.
47. Borges, I.; *Theor. Chem. Acc.* **2008**, *121*, 239.
48. Borges, I.; *Chem. Phys.* **2008**, *349*, 256.
49. Borges, I.; Aquino, A. J.; Barbatti, M.; Lischka, H.; *Int. J. Quantum Chem.* **2009**, *109*, 2348.
50. Borges, I.; Barbatti, M.; Aquino, A. J. A.; Lischka, H.; *Int. J. Quantum Chem.* **2012**, *112*, 1225.
51. Borges, I.; Aquino, A. J. A.; Lischka, H.; *J. Phys. Chem. A* **2014**, *118*, 12011.
52. Becke, A. D.; *J. Chem. Phys.* **1993**, *98*, 5648.
53. Dunning, T. H.; *J. Chem. Phys.* **1989**, *90*, 1007.
54. Feller, D.; *J. Comput. Chem.* **1996**, *17*, 1571.
55. Frisch, M. J.; Trucks, G. W.; Schlegel, H. B.; Scuseria, G. E.; Robb, M. A.; Cheeseman, J. R.; Montgomery, J. A.; Vreven, T.; Kudin, K. N.; Burant, J. C.; Millam, J. M.; Iyengar, S. S.; Tomasi, J.; Barone, V.; Mennucci, B.; Cossi, B.; Scalmani, G.; Rega, N.; Petersson, G. A.; Nakatsuji, H.; Hada, M.; Ehara, M.; Toyota, K.; Fukuda, R.; Hasegawa, J.; Ishida, M.; Nakajima, T.; Honda, Y.; Kitao, O.; Nakai, H.; Klene, M.; Li, X.; Knox, J. E.; Hratchian, H. P.; Cross, J. B.; Adamo, C.; Jaramillo, J.; Gomperts, R.; Stratmann, R. E.; Yazyev, O.; Austin, A. J.; Cammi, R.; Pomelli, C.; Ochterski, J. W.; Ayala, P. Y.; Morokuma, K.; Voth, G. A.; Salvador, P.; Dannenberg, J. J.; Zakrzewski, J.; Dapprich, S.; Daniels, A. D.; Strain, M. C.; Farkas, O.; Malick, D. K.; Rabuck, A. D.; Raghavachari, K.; Foresman, J. B.; Ortiz, J. V.; Cui, Q.; Baboul, A. G.; Clifford, S.; Cioslowski, J.; Stefanov, B. B.; Liu, G.; Liashenko, A.; Piskorz, P.; Komaromi, I.; Martin, R. L.; Fox, D. J.; Keith, T. J.; Al-Laham, M. A.; Peng, C. Y.; Nanayakkara, A.; Challacombe, M.; Gill, P. M. W.; Johnson, B.; Chen, W.; Wong, M. W.; Gonzalez, C.; Pople, J. A.; *Gaussian 03*, *Revision C.02*, Gaussian Inc.: Pittsburgh, 2003.
56. Stone, A. J.; *J. Chem. Theory Comput.* **2005**, *1*, 1128.
57. Lopez, R.; Rico, J. F.; Ramirez, G.; Ema, I.; Zorrilla, D.; *Comput. Phys. Commun.* **2009**, *180*, 1654.
58. Allouche, A. R.; *J. Comput. Chem.* **2011**, *32*, 174.
59. Komorowski, L.; Ordon, P.; *J. Mol. Struct.: THEOCHEM* **2003**, 25.
60. Ordon, P.; Komorowski, L.; *Chem. Phys. Lett.* **1998**, *292*, 22.
61. Levine, I. N.; *Quantum Chemistry*, Prentice Hall: Englewood Cliffs, 1991.
62. Bemm, U.; Ostmark, H.; *Acta Crystallogr., Sect. C: Cryst. Struct. Commun.* **1998**, *54*, 1997.
63. Sorescu, D. C.; Boatz, J. A.; Thompson, D. L.; *J. Phys. Chem. A* **2001**, *105*, 5010.
64. Baum, K.; Bigelow, S. S.; Nguyen, N. V.; Archibald, T. G.; Gilardi, R.; Flippenanderson, J. L.; George, C.; *J. Org. Chem.* **1992**, *57*, 235.
65. Price, S. L.; *Chem. Phys. Lett.* **1985**, *114*, 359.
66. Arunan, E.; Desiraju, G. R.; Klein, R. A.; Sadlej, J.; Scheiner, S.; Alkorta, I.; Clary, D. C.; Crabtree, R. H.; Dannenberg, J. J.; Hobza, P.; Kjaergaard, H. G.; Legon, A. C.; Mennucci, B.; Nesbitt, D. J.; *Pure Appl. Chem.* **2011**, *83*, 1619.
67. Mathieu, D.; *J. Phys. Chem. A* **2013**, *117*, 2253.
68. Politzer, P.; Laurence, P. R.; Abrahmsen, L.; Zilles, B. A.; Sjoberg, P.; *Chem. Phys. Lett.* **1984**, *111*, 75.

*Submitted: November 10, 2014*
*Published online: February 24, 2015*